Asian Journal of Water, Environment and Pollution, Vol. 19, No. 1 (2022), pp. 47-58.
DOI 10.3233/AJW220008

Analysing the Changes in Water Quality of River Ganga Passing Through Urban Cities with Remote Sensing and GIS Support

Kamakshi Singh and Ramakar Jha*
National Institute of Technology, Patna – 80005, India
✉ rjha43@gmail.com

Received January 30, 2021; revised and accepted August 13, 2021

Abstract: River Ganga in India has tremendous self-purification capacity due to its dynamic, turbulent and meandering characteristics. In addition due to the presence of anti-bacterial agents such as Bacteriophages virus killing bacteria and its medicinal properties, the refinement capacity increases. In the present work, water quality samples of river Ganga at Kanpur, Prayagraj, Varanasi, Patna and Bhagalpur were collected and analysed for the years 2017-2019 to assess the change in water quality of the river Ganga in terms of total suspended solids (TSS) and turbidity through remote sensing data and ground observations. The change in spectral reflectance of water along the river in the visible region has been analysed using the Landsat-8 multispectral remote sensing data and water quality samples have been collected from all the sites on the date of pass of Landsat-8 satellite. The results obtained shows that the satellite based remote sensing approach can be effectively used to make qualitative and quantitative estimates of total suspended solids and turbidity using nonlinear equations with high accuracy, even in the absence of field observations.

Key words: Remote sensing, water quality, satellite data, total suspended solids, turbidity, spectral reflectance, nonlinear models

Introduction

Remote sensing approaches to measure inland water quality data has been done since the beginning of the satellite era (Jha et al., 2008a, 2008b, 2008c; Johnson, 1975; Ritchie et al., 1976; Sahoo et al., 2019; Singh and Jha, 2018, 2020). Over this time span, hundreds of peer-reviewed publications have shown promising remote sensing models to estimate the biological, chemical, and physical properties of inland waterbodies (Moore, 1980).

Among all the water quality parameters, total suspended solids (TSS) particles are the most common problem in inland waters such as rivers, lakes, and estuaries (Ritchie et al., 1974). It attenuates the light below the water surface required for aquatic life (Doxaran et al., 2002; Garg et al., 2017; Ritchie et al., 1974). The total suspended solids (TSS) refer to both inorganic as well as organic particles that persist in suspension throughout a river system, especially during the monsoon period. The monitoring of TSS fluctuations has strong implications for biogeochemical cycling in terms of nutrient transport, heavy metal loading, global carbon budgets and light conditions (Rügner et al., 2013). The TSS attenuates the light below the water surface and its spectral signatures can vary significantly based on the particle size and composition of organic to inorganic materials (Novo et al., 1989; Spyrakos et al., 2017). The organic-dominated systems derive their spectral signatures from algae concentrations

*Corresponding Author

and can share the pronounced absorption features and backscatter peaks described above for chlorophyll (Shi et al., 2013). The location of the spectral maximum moves from around 550 nm into the red or near-infrared wavelengths due to an increase in inorganic TSS concentrations within a waterbody. TSS concentrations can be correlated with various optically inactive water quality parameters such as the concentration of phosphorous, mercury, and other metals at local scales (Telmer et al., 2006).

Moreover, turbidity is another important optical property of water, which increases with an increase in the concentration of suspended solids or sediments in water (Garg et al., 2017; Ritchie et al., 1976; Sebasti_a-Frasquet et al., 2019). Turbidity enhances the opacity of water, which again hampers aquatic life (Geuttler et al., 2013; Sebasti_a-Frasquet et al., 2019; Quang et al., 2017). The turbidity regulates freshwater ecosystems through light attenuation and control over depth (Mazumder and Taylor, 1994). Most commonly, Secchi Disk depth is used as relative measure of turbidity. The concept of Secchi Disk depth was developed more than 150 years ago to quantify the maximum visible depth of a white and black disk lowered into a waterbody (Wernand, 2010). In comparison, turbidity is an explicit measurement of light scattering within a water column caused by suspended and dissolved particles.

In the past, a number of studies have been carried out to examine the role of turbidity in thermal stratification, lake metabolism (Obrador et al., 2014; Schwarz and Hawes, 1997), and biodiversity (Bilotta and Brazier, 2008). Remote sensing analysis of turbidity uses band ratios and wavelengths that include the red spectrum as main input data (Baban, 1993; Bayley et al., 2007; Hicks et al., 2013; McCullough et al., 2012; Nelson et al., 2003; Rose et al., 2017; Wu et al., 2008).

The remote sensing satellite data reflectance in the visible region (red region) increases with an increase in sediments in the water or turbidity and can be used to assess the water quality of inland water (Caballero et al., 2019; Doxaran et al., 2002; Garg et al., 2017; Gholizadeh et al., 2016; IOCCG, 2000; Moore, 1980; Pavelsky and Smith, 2009; Ritchie et al., 1976; Toming et al., 2016; Sebasti_a-Frasquet et al., 2019).

In the present study, an attempt has been made to use satellite based remote sensing approach effectively to make qualitative and quantitative estimates of total suspended solids and turbidity using the different commonly used non-linear models.

The Study Area and Data Collection

The study area includes the Ganga river basin extending from Kanpur to Bhagalpur (Figure 1), which includes the cities of Kanpur, Prayagraj, Varanasi, Patna and Bhagalpur. The sampling in Kanpur is done at Balu ghat and Gola ghat. In Prayagraj, the sampling is done at the Sangam mela ground having three points, i.e., Ganga river and Sangam. At the holy city of Varanasi, two points of sampling were selected, one being the downstream (Dashashwamedh Ghat) and the second being the upstream (Assi Ghat). In Patna, Digha ghat and Gandhi Ghat was selected. For Bhagalpur, two points were selected for sampling i.e. Kuppa Ghat and Barrari Ghat.

Figure 1: The location map of the study area.

The water quality samples were collected from Kanpur, Prayagraj (Allahabad), Varanasi, Patna & Bhagalpur on monthly basis on the dates coinciding with the satellite pass dates (±2day) of LANDSAT-8 for the year 2017-2019. The Landsat-8 satellite data were collected from the USGS website (http://earthexplorer.usgs.gov/) and atmospheric correction, as well as reflectance correction, were made before processing of the image. Earth Explorer is an online interface to collect the satellite data developed by USGS. Data of the study region were collected according to the path and row of the Landsat-8 satellite for the following dates (Table 1):

Methodology

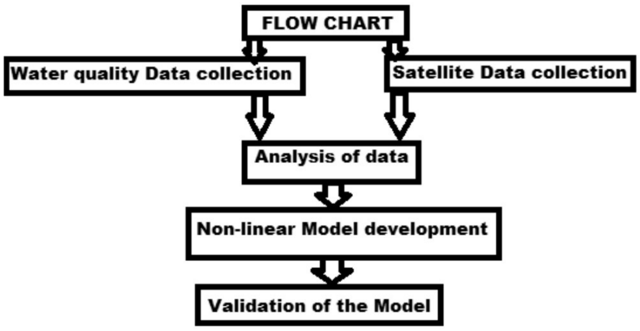

Water Quality Data Collection and Analysis Procedure

The sampling was done on monthly basis on the dates coinciding with the satellite pass dates (±2 days) of LANDSAT-8 from Kanpur, Prayagraj, Varanasi, Patna & Bhagalpur. The grab sampling method was applied for collecting the samples. Samples were collected within 5 m from the river bank at a depth of ~0.5 m in Teflon bottles of 2 L. The samples were transported and stored at 4°C until analysis. The water quality parameters, total suspended solids (TSS) and turbidity were measured in the laboratory by the standard method (APHA, 2017).

The nylon membrane filter papers were incubated under cool and dark conditions for 5 hrs at 100°C and weighted before filtering. Water samples from each sampling site are filtered through Whatman GF/F filters of pore size of 0.4 µm and diameter 47 mm. The filtrates were then again incubated under cool and dark conditions for 5 hrs at 40°C and weighed.

To measure the turbidity, a Nephelometric Turbidity meter was used. The instrument was first calibrated with a known sample each time and then the samples collected from upstream and downstream locations of Kanpur, Prayagraj, Varanasi, Patna and Bhagalpur were tested to measure turbidity in NTU units.

Satellite Data Collection and Analysis Procedure

In the present work, Landsat 8 satellite data collected from the USGS website were used for obtaining NDWI, NDTI and multiple linear correlations for total suspended solids and turbidity.

Water Reflectance (R_{rs}) of Band 8 (0.842 µm) for TSS estimation

To create the best band ratio model for SPM estimation, 2-B/3-B/4-B models incorporating all possible combinations of B1 to B8 of Sentinel-2 were tested using linear, quadratic, logarithmic, power, and exponential functions. Finally, the best model, i.e., the 1-B model of Band 8 (NIR) with higher R^2 were selected.

$$\text{Landsat} - 8\ (0.842) = \text{Rrs (NIR)} \qquad (1)$$

Normalised Difference Turbidity Index

It has been reported that the red region reflectance increases with an increase in turbidity. Therefore, the red and green bands were used to enhance the image for turbidity and the normalised difference turbidity index (NDTI) is an index of Red and Green Bands indicating turbidity.

$$\text{NDTI} = \frac{(\text{Red } (0.61\text{-}0.68\ \mu\text{m})\text{- Green}(0.5\text{- }0.59\ \mu\text{m}))}{(\text{Red } (0.61\text{-}0.68\ \mu\text{m})\text{+ Green}(0.5\text{- }0.59\ \mu\text{m}))}$$

Landsat 8 (Band4 – Band3)/(Band4 + Band3) (2)

Table 1: Landsat-8 satellite data collection details at each sampling stations

Sampling Station	*(Path/row)*	*Dates for Satellite Data collection*
Kanpur	144/42	29/04/2017, 06/05/2017, 07/06/2017, 15/10/2017,
Prayagraj	143/42	13/11/2017, 29/12/2017, 23/01/2018, 15/02/2018,
Varanasi	142/42	19/03/2018, 21/03/2018, 15/04/2018, 08/05/2018,
Patna	141/42	07/06/2018, 25/06/2018, 15/10/2018, 16/11/2018,
Bhagalpur	140/42	16/12/2018

The higher value of turbidity provides a high value of NDTI and vice versa.

Non-Linear Models

Many non-linear and linear models were tested for their performance to estimate Total suspended solids (TSS) and turbidity. However, the five models, namely the Weibull model, MMM model, exponential model, power model and rational model, provided the best results. The governing equations used in the model are as given below.

Weibull Model

$$Y = a - b \times e^{(-c \times X^d)} \tag{3}$$

Sigmoid Function (MMM Model)

$$Y = \frac{a \times b + c \times X^d}{b + X^d} \tag{4}$$

Exponential Model

$$Y = a \times e^{(b \times X)} \tag{5}$$

Power Model

$$Y = a \times x^b \tag{6}$$

Rational Model

$$\text{Y} = \frac{a + b \times X}{1 + c \times X + d \times X^2} \tag{7}$$

Results and Discussion

In the present study, an effort has been made to study total suspended solids and turbidity using remote sensing data, and develop a relationship between the satellite data and water quality samples collection during satellite pass from the field. For the analysis, two locations at the bank of river Ganga at Kanpur, Prayagraj, Varanasi, Patna and Bhagalpur were identified and water quality samples on monthly basis were collected on the date of pass of Landsat-8 satellite. River Ganga is the most sacred river in India, and the samples of this river collected from these cities show that the water quality in the river is not fit for drinking purposes. Moreover, it is not suitable for bathing as well at certain locations. The results obtained using different remote sensing indices discussed above and the non-linear equations are given below.

Water Reflectance (R_{rs}) of Band 8 (0.842 µm) for TSS Estimation

The total suspended solids (TSS) is a primary measure of water quality (European Union, 2008) and is of interest to the bio-optical community (Nechad et al., 2010). Obtaining TSS data from high-resolution remote sensing satellites offers a cheap and regular data source. Eq. (1) has been used to obtain the TSS values using Landsat-8 satellite data for the years 2017, 2018 and 2019 for all the cities as shown in Figure 2.

For Figure 2, the change in reflectance in each NIR band was observed. Maximum TSS was observed at Kanpur in the year 2019 followed by Bhagalpur. At Patna and Varanasi, TSS was moderate; whereas at Prayagraj, it is found to be minimum in comparison to other cities.

Normalised Difference Turbidity Index

Eq. (2) has been used to assess the NDTI values using the red and green bands satellite data of Landsat-8. The higher value of turbidity provides a high value of NDTI and vice versa.

As shown in Figure 3, significant turbidity was noticed in Kanpur area. The river stretches at Sangam and Prayagraj showed major changes in turbidity. At this location, Ganga is shallow as compared to the Yamuna, and brings more sediments along with it. Furthermore, heavy pilgrimage activity at this location keeps water turbid. The river stretch analysis near Varanasi, again showed turbidity, as reflectance throughout the visible and NIR region due to pilgrimage activities and disposal of pollutants in the river Ganga without prior treatment.

At Patna, the turbidity is found to be very high due to the influx of sediment from Ghaghra, Sone and Gandak river systems in addition to the sediments and pollutants coming from Kanpur and Varanasi. The same situation is found at Bhagalpur too.

Non Linear Models

Four non-linear models, namely the Weibull model, MMM model, exponential model, power model and rational model, were tested for their applicability to assess the TSS and turbidity at Kanpur, Prayagraj, Varanasi, Patna and Bhagalpur. The results obtained are discussed below.

Total Suspended Solid (TSS) Estimation

Using Eqs (3), (4), (5), (6) and (7), the TSS was assessed by considering Landsat NIR data (remote sensing reflectance) as input. The developed equations for all five models are given below.

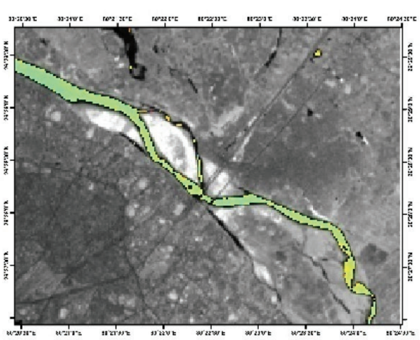

(a) November 2017

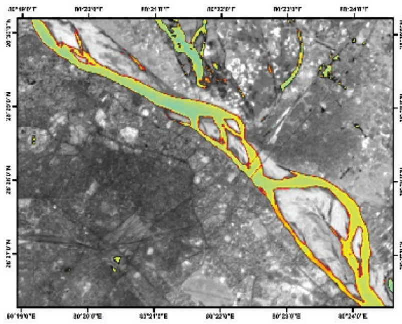

(b) November 2018

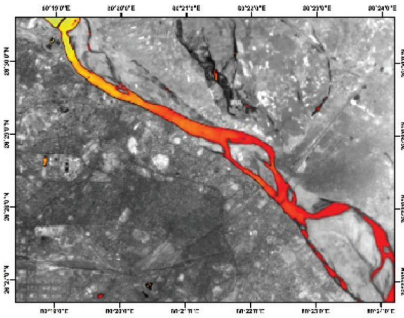

(c) November 2019

Kanpur

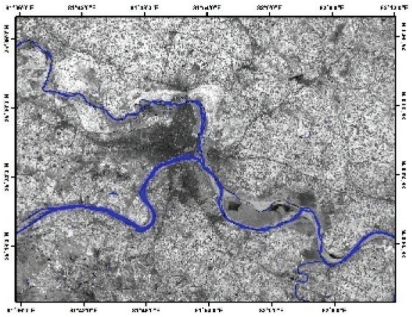

(a) November 2017

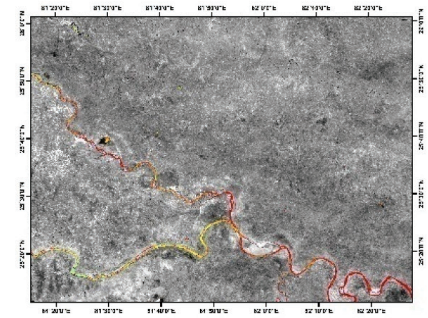

(b) November 2018

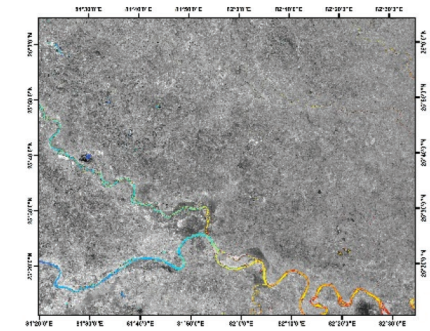

(c) November 2019

Prayagraj

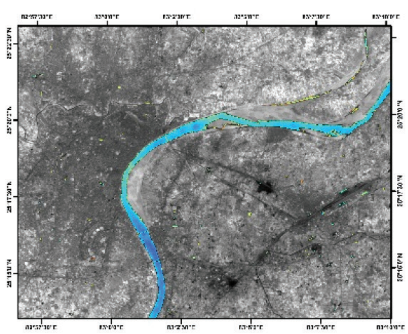

(a) November 2017

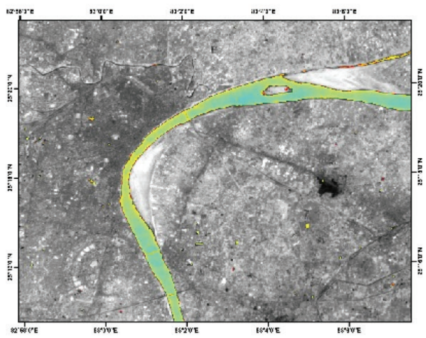

(b) November 2018

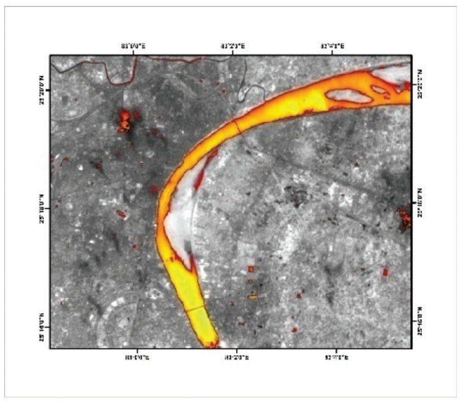

(c) November 2019

Varanasi

Figure 2: (*Contd.*)

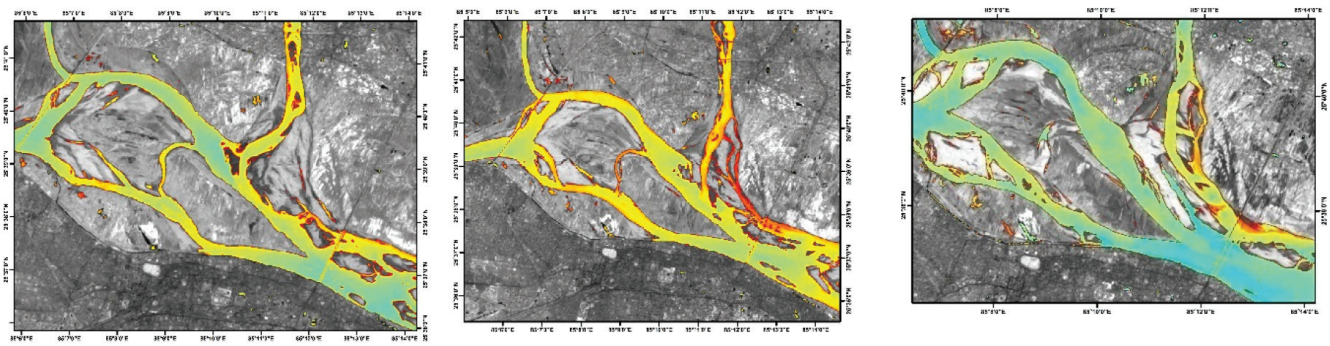

(a) November 2017 (b) November 2018 (c) November 2019

Patna

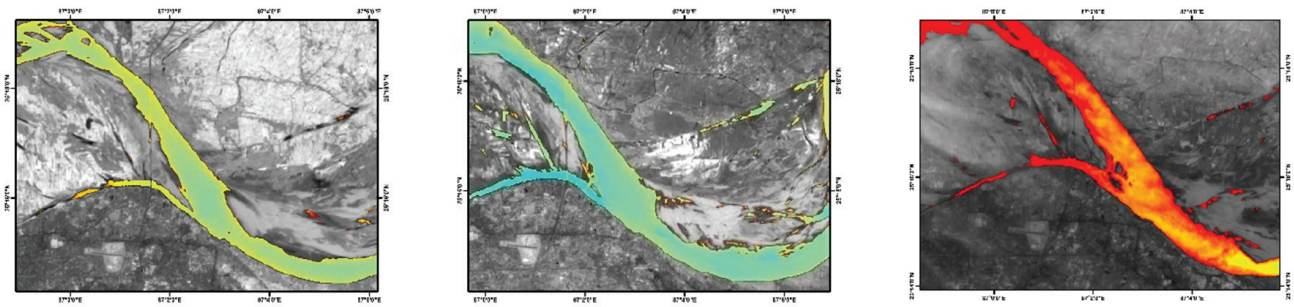

(a) November 2017 (b) November 2018 (c) November 2019

Bhagalpur

Figure 2: Water reflectance of Landsat-8 Band 8 for TSS observation.

Weibull Model

$$TSS = 6637.29 - 6605.91 \times e^{(-0.00000969 \times R_{rs}^{5.439})} \quad (8)$$

Where TSS= Total suspended solids, and Rrs= Remote sensing reflectance of NIR

Sigmoid Function (MMM Model)

$$TSS = \frac{(13.0655 \times 199.076 + 421.26 \times R_{rs}^{3.1})}{(199.076 + R_{rs}^{3.1})} \quad (9)$$

Exponential Model

$$TSS = 6.179 \times e^{(0.775 \times Rrs)} \quad (10)$$

Power Model

$$TSS = 5.67 \times x^{2.24 \times Rrs} \quad (11)$$

Rational Model

$$TSS = \frac{289.861 - 75.977 \times R_{rs}}{1 + 2.341 \times R_{rs} - .715 \times R_{rs}^2} \quad (12)$$

Using Eqs (8), (9), (10), (11) and (12), the results obtained from Kanpur, Prayagraj, Varanasi, Patna and Bhagalpur were combined to increase the number of data sets in addition to individual analysis. The results obtained are shown in Figure 4. It is observed that for estimating TSS, all the non-linear models developed using Eqs (8) to (12), provide a high coefficient of determination (R^2) values, except rational model. Any of the methods can be used to estimate the TSS if reflectance values are obtained using Landsat-8 NIR data.

Turbidity Estimation

Using Eqs (3), (4), (5), (6) and (7), the turbidity was assessed by considering Landsat-8 data by developing normalised difference turbidity index (NDTI) as input. The developed equations for all five models are given below.

Weibull Model

$$\text{Turbidity} = 28.482 - 17.511 \times e^{(-2.872 \times \text{NDTI}^{-2.794})} \quad (13)$$

Sigmoid Function (MMM Model)

$$\text{Turbidity} = \frac{11.445 \times .203 + 28.538 \times \text{NDTI}^{-3.225}}{.203 + \text{NDTI}^{-3.225}} \quad (14)$$

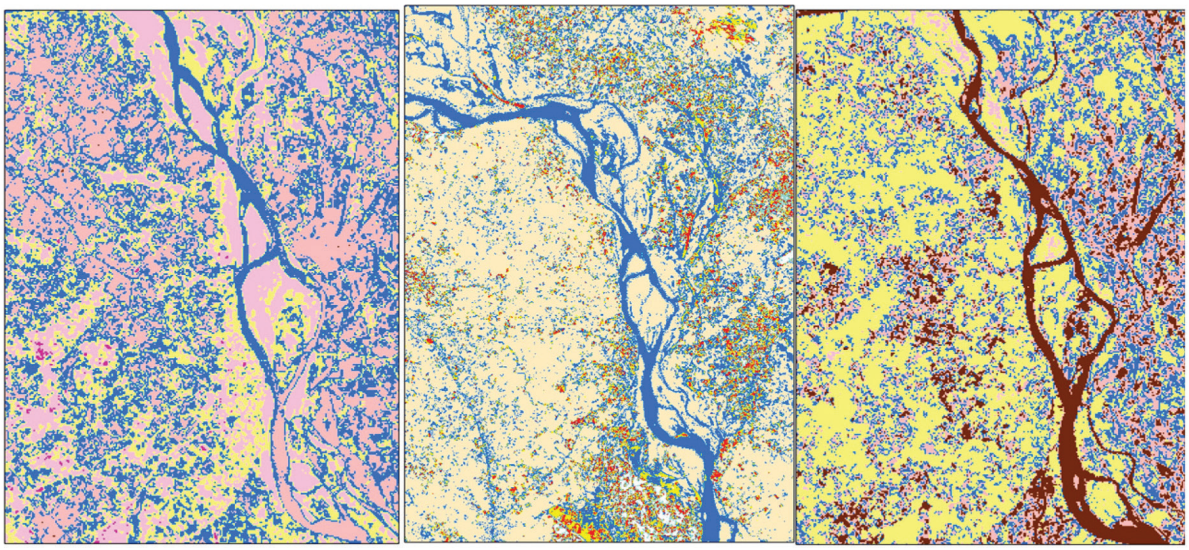

(a) November 2017 (b) November 2018 (c) November 2019

Kanpur

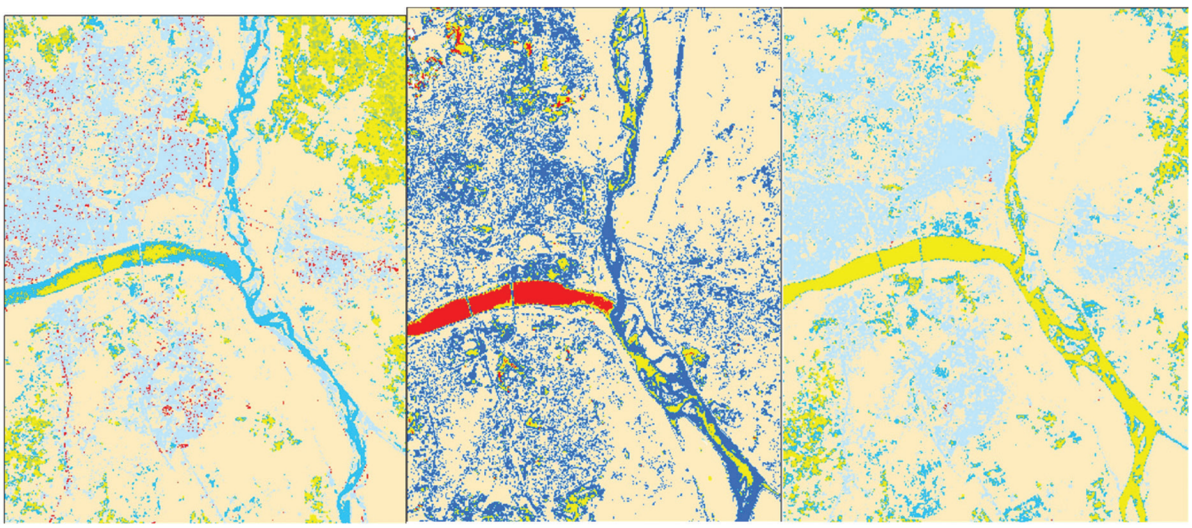

(a) November 2017 (b) November 2018 (c) November 2019

Prayagraj

Figure 3: (*Contd.*)

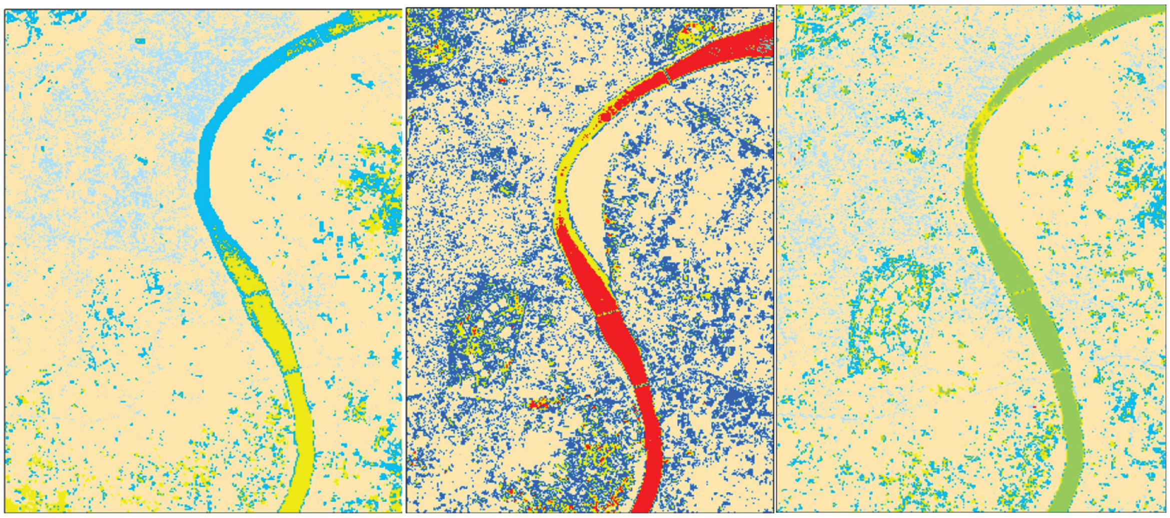

(a) November 2017 (b) November 2018 (c) November 2019

Varanasi

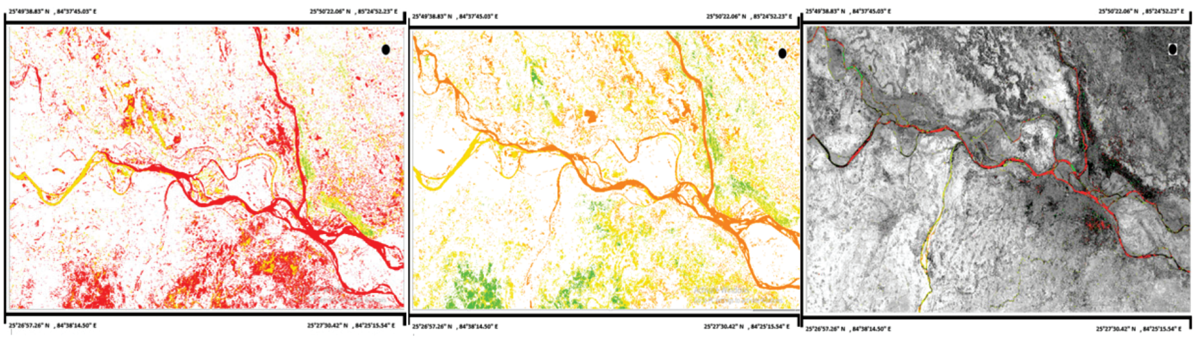

(a) November 2017 (b) November 2018 (c) November 2019

Patna

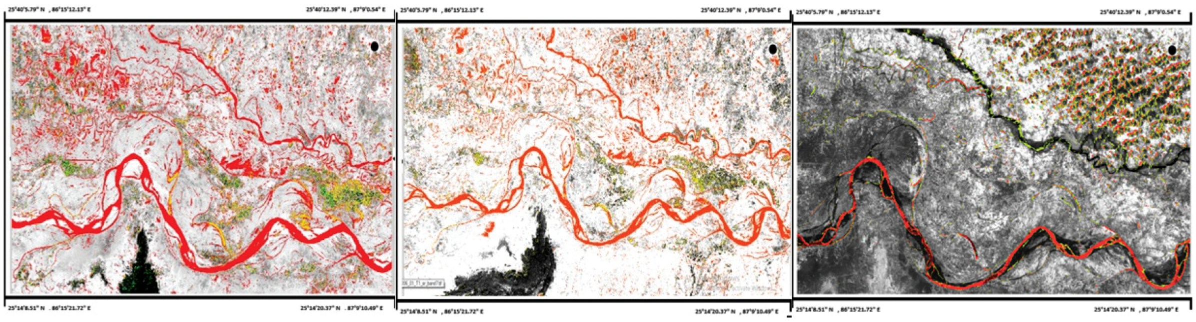

(a) November 2017 (b) November 2018 (c) November 2019

Bhagalpur

Figure 3: NDTI using Landsat-8 satellite for turbidity observation.

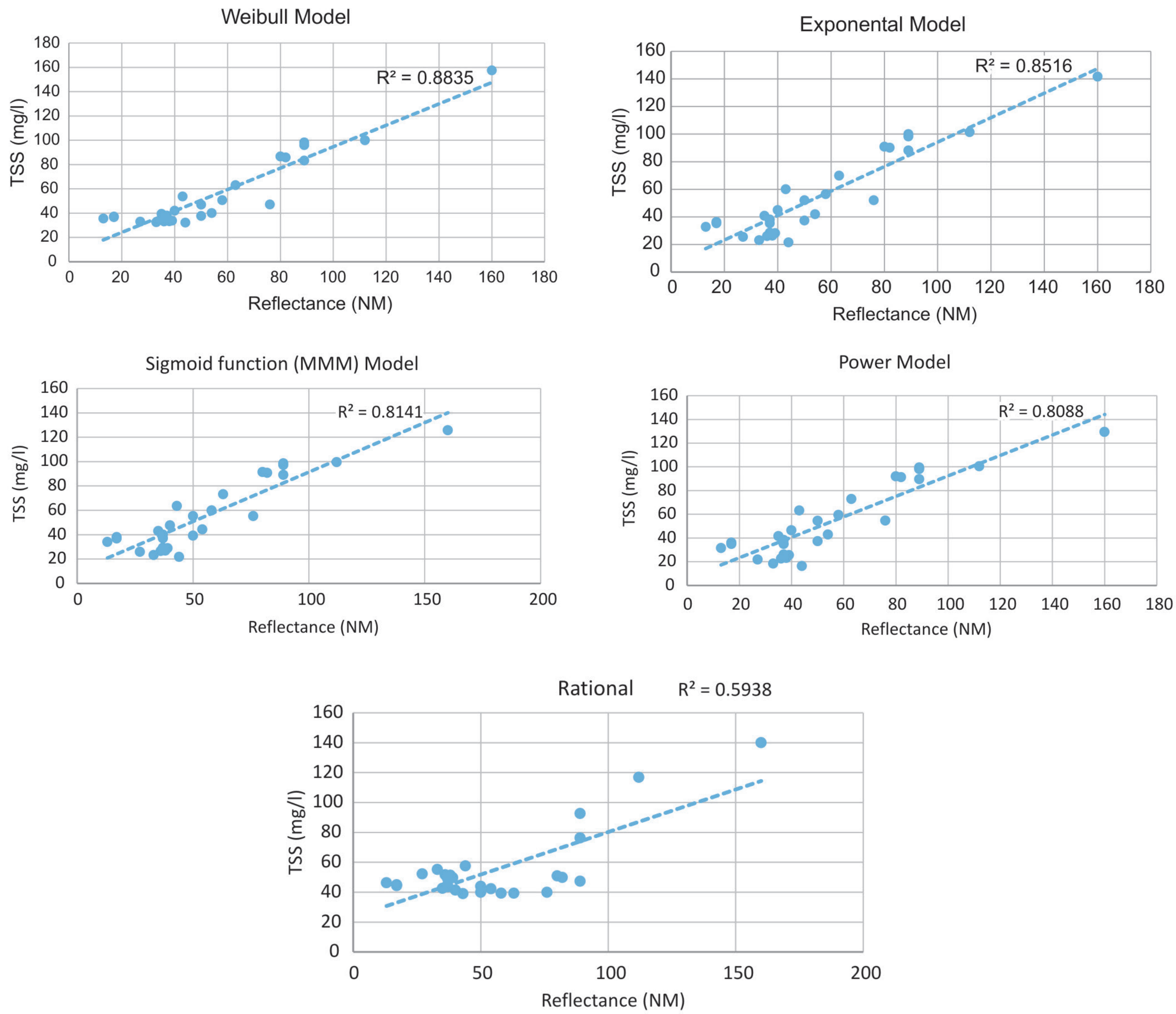

Figure 4: Estimating total suspended solids using NIR remote sensing satellite data.

Exponential Model

$$\text{Turbidity} = 21.275 \times e^{(-.0991 \times \text{NDTI})} \quad (15)$$

Power Model

$$\text{Turbidity} = 18.6 \times x^{(-2.6 \times \text{NDTI})} \quad (16)$$

Rational Model

$$\text{Turbidity} = \frac{(31.865 - 1.865 \times \text{NDTI})}{1 + 0.43 \times \text{NDTI} - .042 \times \text{NDTI}^2} \quad (17)$$

Using equations (13), (14), (15), (16) and (17), the results obtained for Kanpur, Prayagraj, Varanasi, Patna and Bhagalpur were combined to increase the number of data sets in addition to individual analysis. The results obtained are shown in Figure 5. It is observed that for estimating turbidity, all the non-linear models developed using Eqs (13) to (17), provide a high coefficient of determination (R^2) values, except the Exponential model. Any of the methods can be used to estimate the turbidity, if reflectance values are obtained using Landsat-8 NDTI data sets.

Conclusions

TSS and turbidity are two very important optical variables of remote sensing applications, which provide useful information on the water quality of inland water bodies on real time basis.

Both the variables reduce the energy required for aquatic growth, respiration and photosynthesis.

In the present study, the spatial and temporal change in turbidity has been analysed along the Ganga River during the years 2017 to 2019 through remote sensing and ground observations. The major cities located along the river Ganga were selected for the study. They are Kanpur, Prayagraj, Varanasi, Patna and Bhagalpur.

Initially, the change in total suspended solids (TSS) has been analysed in terms of change in reflectance in the NIR region of Landsat-8 data. It has been reported in the literature that with the increase in TSS the reflectance increases and vice versa. Similar results were found in the present study at all five cities. Moreover, the temporal change study showed that reflectance

in the NIR region the values have increased at each location from the year 2017-2019. Maximum TSS was observed at Kanpur in the year 2019 followed by Bhagalpur. At Patna and Varanasi, TSS was moderate whereas at Prayagraj, it is found to be minimum in comparison to other cities.

The results obtained using NDTI band ratio technique also confirmed that the turbidity is high at Kanpur, Bhagalpur, Patna and Varanasi. The river stretch at

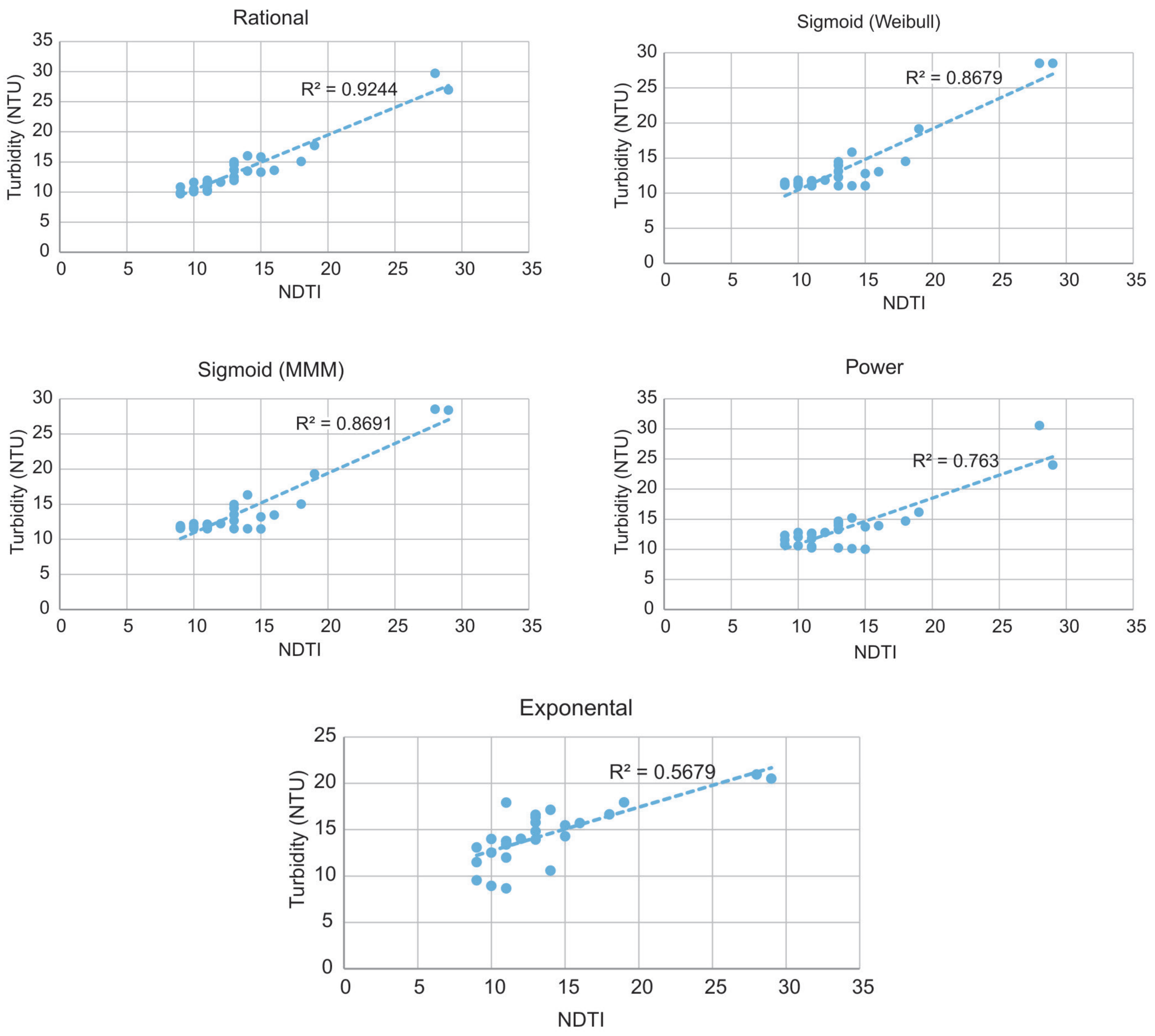

Figure 5: Estimating turbidity using NDTI of remote sensing satellite data.

Sangam and Prayagraj showed major changes in turbidity. At this location, Ganga is shallow as compared to the Yamuna and so brings more sediments along with it. Further, heavy pilgrimage activity at this location keeps the water constantly turbid. The analysis at the river stretch near Varanasi, again showed turbidity, as reflectance throughout the visible and NIR region due to pilgrimage activities and disposal of pollutants in the river Ganga without prior treatment. At Patna, the turbidity is found to be very high due to the influx of sediment from Ghaghra, Sone and Gandak river systems in addition to the sediments and pollutants coming from Kanpur and Varanasi. The same situation is found at Bhagalpur too.

It is observed that for estimating TSS and turbidity, all the non-linear models developed in the present work are very useful for planners and field engineers with high accuracy. The rational model was showing poor estimates of TSS, where as exponential models showed poor results in estimating turbidity.

The methods used are very promising and can be used for water quality monitoring and modeling using satellite data.

Acknowledgements

The authors wish to thank all the officials of SAC, ISRO Ahmedabad for sponsoring the project. The authors also with to than the Institute for logistic support.

References

Baban, S.M.J. (1993). Detecting water quality parameters in the Norfolk broads, U.K., using Landsat imagery. *InternationalJournal of Remote Sensing*, **14**: 1247-1267. https://doi.org/10.1080/01431169308953955

Bayley, S.E., Creed, I.F., Sass, G.Z. and A.S. Wong, (2007). Frequent regime shifts in trophic states in shallow lakes on the Boreal Plain: Alternative "unstable" states? *Limnology Oceanography*, **52:** 2002-2012. https://doi.org/10.4319/lo.2007.52.5.2002

Bilotta, G.S. and R.E. Brazier (2008). Understanding the influence of suspended solids on water quality and aquatic biota. *Water Research*, **42:** 2849-2861. DOI: 10.1016/j.watres.2008.03.018

Caballero, I., Stumpf, R.P. and A. Meredith (2019). Preliminary assessment of turbidity and chlorophyllimpact on bathymetry derived from Landsat-8A and Sentinel-3A satellites in South Florida. *Remote* Sensing, **11(6):** 645. https://doi.org/10.3390/rs11060645

Doxaran, D., Froidefond, J.M., Lavender, S. and P. Castaing (2002). Spectral signature of highly turbid waters Application with SPOT data to quantify suspended particulate matter concentrations. *Remote Sensing of Environment*, **81(1):** 149-161. https://doi.org/10.1016/S0034-4257(01)00341-8

Garg, V., Senthil Kumar, A., Aggarwal, S.P., Kumar, V., Dhote, P.R., Thakur, P.K., Nikam, B.R., Sambare, R.S., Siddiqui, A. and P.R. Muduli (2017). Spectral similarity approach for mapping turbidity of an inland waterbody. *Journal of Hydrology,* **550:** 527-537. 10.1016/j.jhydrol.2017.05.039

Gholizadeh, M.H., Melesse, A.M. and L. Reddi (2016). A comprehensive review on water quality parameters estimation using remote sensing techniques. *Sensors*. **16(8):** 1298. https://doi.org/10.3390/s16081298

Geuttler, F.N., Niculescu, S. and F. Gohin (2013). Turbidity retrieval and monitoring of Danube Delta waters using multi-sensor optical remote sensing data: an integrated view from the delta plain lakes to the western–northwestern Black Sea coastal zone. *Remote Sensing and Environment*, **132:** 86-101. 10.1016/j.rse.2013.01.009

Hicks, B.J., Stichbury, G.A., Brabyn, L.K., Allan, M.G. and S. Ashraf (2013). Hindcasting water clarity from Landsat satellite images of unmonitored shallow lakes in the Waikato region, New Zealand. *Environment Monitoring Assessment*, 185: 7245-7261. DOI 10.1007/s10661-013-3098-2

Jha, R., Sharma, K.D. and V.P. Singh (2008a). Critical appraisal of methods for the assessment of environmental flows and their application in Two river systems of India. *KSCE Journal of Civil Engineering*, **12(3):** 213-219. https://doi.org/10.1007/s12205-008-0213-y

Jha, R. and V.P. Singh (2008b). Analytical water quality model for Biochemical Oxygen Demand simulation in River Gomti of Ganga Basin, India. *KSCE Journal of Civil Engineering*, **12(2):** 141-147. https://doi.org/10.1007/s12205-008-0141-x

Jha, R. and V.P. Singh (2008c). Evaluation of river water quality by entropy.*KSCE Journal of Civil Engineering*, **12(1):** 61-69. https://doi.org/10.1007/s12205-008-8061-3

Johnson, R.W. (1975). Quantitative sediment mapping from remotely sensed multispectral data. *In:* Shahrokhi F, editor. Remote sensing of earth resources, Vol. IV. Tullahoma (TN): The University of Tennessee Space Institute; p. 565–576.

Klemas, V., Borchardt, J.F. and W.M. Treasure (1971). Suspended sediment observations from ERTS1. *Remote Sensing of* Environment, **2:** 205-221. https://doi.org/10.1016/0034-4257(71)90094-0

Kritikos, H., Yorinks, L. and H. Smith (1974). Suspended solids analyses using ERT-A data. *Remote Sensing of Environment,* **3(1):** 69-78.

McCullough, I.M., Loftin, C.S. and S.A. Sader (2012). Combining lake and watershed characteristics with

Landsat TM data for remote estimation of regional lake clarity. *Remote Sensing of Environment*, **123:** 109-115. DOI:10.1016/j.rse.2012.03.006

Moore, G.K. (1980). Satellite remote sensing of water turbidity. *Hydrological Sciences Journal,* **25(4):** 407-421.

Nelson, S.A.C., Soranno, P.A., Cheruvelil, K.S., Batzli, S.A. and D.L. Skole (2003). Regional Assessment of lake water clarity using satellite remote sensing. *Journal of Limnology*, **62:** 27-32. https://doi.org/10.4081/jlimnol.2003.s1.27

Novo, E.M., Hansom, J.D. and P.J. Curran (1989). The effect of sediment type on the relationship between reflectance and suspended sediment concentration. *International Journalof Remote Sensing*, **10:** 1283-1289. https://doi.org/10.1080/01431168908903967

Obrador, B., Staehr, P.A. and J.P.C. Christensen (2014). Vertical patterns of metabolism in three contrasting stratified lakes. *Limnology Oceanography*, **59:** 1228-1240. https://doi.org/10.4319/lo.2014.59.4.1228

Pavelsky, T.M. and L.C. Smith (2009). Remote sensing of suspended sediment concentration, flow velocity, and lake recharge in the Peace-Athabasca Delta, Canada. *Water Resources Research,***45(11):** W11417. https://doi.org/10.1029/2008WR007424

Quang, N.H., Sasaki, J., Higa, H. and N.H. Huan (2017). Spatiotemporal variation of turbidity based on Landsat 8 OLI in Cam Ranh Bay and Thuy Trieu Lagoon, Vietnam. *Water*, **9(8):** 570. https://doi.org/10.3390/w9080570

Ritchie, J.C., McHenry, J,R., Schiebe, F.R. and R.B. Wilson (1974). The relationship of reflected solar radiation and the concentration of sediment in surface water of reservoirs. *In:* Shahrokhi F, 1194 V. Garget al.. editor. Remote sensing of earth resources, Vol. III. Tullahoma (TN): The University of Tennessee Space Institute; p. 52–72.

Ritchie, J., Schiebe, F.R. and J.R. McHenry (1976). Remote sensing of suspended sediments in surface waters. *Photogrammetry Engineering in Remote Sensing*, **42(12):** 1539–1545.

Rose, K.C., Greb, S.R., Diebel, M. and M.G. Turner (2017). Annual precipitation regulates spatial and temporal drivers of lake water clarity. *Ecological Application*, **27:** 632-643. DOI: 10.1002/eap.1471

Rügner, H., Schwientek, M., Beckingham, B., Kuch, B. and P. Grathwohl (2013). Turbidity as a proxy for total suspended solids (TSS) and particle facilitated pollutant transport in catchments. *Environmental Earth Science,* **69:** 373-380. DOI:10.1007/s12665-013-2307-1

Sahoo, B.B., Jha, R., Singh, A. and D. Kumar (2019). Application of support vector regression for modeling low flow time series. *KSCE Journal of Civil Engineering,* **23(2):** 923-934. https://doi.org/10.1007/s12205-018-0128-1

Schwarz, A.M. and I. Hawes (1997). Effects of changing water clarity on characean biomass and species composition in a large oligotrophic lake. *Aquatic Botany*, **56:** 169-181. https://doi.org/10.1016/S0304-3770(96)01114-X

Sebasti_a-Frasquet M.T, Aguilar-Maldonado, J.A., Santamarıa-Del, Angel, E. and J. Estornell (2019). Sentinel 2 analysis of turbidity patterns in a coastal lagoon. *Remote Sensing,* **11**(24): 2926. https://doi.org/10.3390/rs11242926

Shi, K., Li, Y., Li, L. and H. Lu (2013). Absorption characteristics of optically complex inland waters: Implications for water optical classification. *Journal of Geophysical Research Bio-geoscience*, **118:** 860-874. https://doi.org/10.1002/jgrg.20071

Singh, K. and R. Jha (2018). Assessment of water quality in River Ganga at Patna, India. Hydraulics, Water Resources and Coastal Engineering: Groundwater and water quality. Springer USA Book Volume 5. Editors: Ramakar Jha, V. P. Singh, Vivekananad Singh, L.B. Roy and Roshni T., p- 40-48

Singh, K. and R. Jha (2020).Water quality of river ganga using remote sensing and GIS techniques – A review. ASCE Conference, Kolkata India. 2-4 March 2020.

Spyrakos, E., O'Donnell, R., Hunter, P.D., Miller, C., Scott, M., Simis, S.G.H., Neil, C., Barbosa, C.C.F., Binding, C.E. and S. Bradt (2017). Optical types of inland and coastal waters. *Limnology Oceanography*, **63:** 846-870. https://doi.org/10.1002/lno.10674

Telmer, K., Costa, M., Angélica, R.S., Araujo, E.S., and Y. Maurice (2006). The source and fate of sediment and mercury in the Tapajos River, Para, Brazilian Amazon: Ground- and space-based evidence. *Journal of Environment Management*, **81:** 101-113. DOI: 10.1016/j.jenvman.2005.09.027

Toming, K., Kutser, T., Laas, A., Sepp, M., Paavel, B. and T. Noges (2016). First experiences in mapping lake water quality parameters with Landsat-8 MSI imagery. *Remote* Sensing, **8(8):** 640. https://doi.org/10.3390/rs8080640

Wu, G., De Leeuw, J., Skidmore, A.K., Prins, H.H.T. and Y. Liu (2008). Comparison of MODIS and Landsat TM5 images for mapping tempo–spatial dynamics of Secchi disk depths in Poyang Lake National Nature Reserve, China. *International Journal of Remote Sensing*, **29:** 2183-2198. https://doi.org/10.3390/rs11020177